



Transient Condensation of Vapor Using a Direct Simulation Monte Carlo Method

M. El-Afify, M.L. Corradini

October 1988

UWFDM-779

Presented at the 8th Topical Meeting on the Technology of Fusion Energy, 9–13 October
1988, Salt Lake City UT.

FUSION TECHNOLOGY INSTITUTE

UNIVERSITY OF WISCONSIN

MADISON WISCONSIN

DISCLAIMER

This report was prepared as an account of work sponsored by an agency of the United States Government. Neither the United States Government, nor any agency thereof, nor any of their employees, makes any warranty, express or implied, or assumes any legal liability or responsibility for the accuracy, completeness, or usefulness of any information, apparatus, product, or process disclosed, or represents that its use would not infringe privately owned rights. Reference herein to any specific commercial product, process, or service by trade name, trademark, manufacturer, or otherwise, does not necessarily constitute or imply its endorsement, recommendation, or favoring by the United States Government or any agency thereof. The views and opinions of authors expressed herein do not necessarily state or reflect those of the United States Government or any agency thereof.

**Transient Condensation of Vapor Using a
Direct Simulation Monte Carlo Method**

M. El-Afify, M.L. Corradini

Fusion Technology Institute
University of Wisconsin
1500 Engineering Drive
Madison, WI 53706

<http://fti.neep.wisc.edu>

October 1988

UWFDM-779

Presented at the 8th Topical Meeting on the Technology of Fusion Energy, 9–13 October 1988, Salt Lake City UT.

TRANSIENT CONDENSATION OF VAPOR USING A DIRECT SIMULATION MONTE CARLO METHOD

M.M. El-Afify and M.L. Corradini
Department of Nuclear Engineering and Engineering Physics
University of Wisconsin, Madison, WI 53706-1687
(608) 263-4447

ABSTRACT

Vapor is produced from the ICF event as the x-ray energy is deposited at the first wall of the reactor. This vapor must condense back onto the first wall in a timely fashion ($\ll 1$ s) to establish the necessary conditions for beam propagation and the next ICF event. Transient condensation of vapor is studied on the basis of the Boltzmann equation using a direct simulation Monte Carlo Method. The method describes the molecular behavior of continuum mechanics transition flows in a way consistent with the Boltzmann equation. The thermal resistance of the condensed film is included in the flow representation using a laminar Nusselt analysis to determine the interface temperature of the condensed film. The condensate mass flux in a quasi-steady state is computed and compared with a number of analytical models and experimental data. The results are consistent qualitatively with the experimental data of mercury condensation on a vertical plate.

INTRODUCTION

In the past several years, the study of transient condensation of a vapor onto a liquid (or solid) surface has received considerable attention especially in the design of liquid metal cooled ICF reactors.^{1,2} Vapor is produced from the ICF event as x-ray and target debris energy is deposited at the first wall of the reactor cavity. In some designs, the first wall is protected with a liquid metal film which is also used for cooling and breeding purposes. This vapor, once produced, must condense back onto the first wall in a timely fashion ($\ll 1$ s) to establish the necessary conditions for beam propagation and the next ICF event. The condensation occurring under these circumstances is at very low vapor densities where the resistance to mass transfer occurs not only in the condensate film but also in the diffusion of the vapor to the interface.

Various models had been developed using kinetic theory arguments to relate the properties of the liquid and vapor phases at the immediate vicinity of the interface, to the net mass transfer rate between the phases. Such models have considered pure vapor condensation as well as condensation in the presence of a noncondensable gas. In this work, we present a unique model for pure vapor condensation using the Direct Simulation Monte Carlo method (DSMC). Such a model is able to predict the qualitative behavior of condensation, while the other analytical models failed to predict such qualitative behavior. In DSMC method, the molecules are allowed to move and collide among themselves. The two processes are decoupled by computing collisions appropriate to a small time step, Δt_m , and their instantaneous velocities. The collisions are represented in a way consistent with the collision frequency of hard sphere molecules.

PROBLEM STATEMENT

In developing our model for condensation we considered the following conceptual picture. Initially, a solid surface is in equilibrium with a pure vapor occupying the half space at an initial temperature T_∞ and initial pressure P_∞ . At zero time, the surface temperature discontinuously changes to T_w , and is kept at T_w throughout the formation of the condensate film on the wall. The calculations are time dependent to determine the dynamic behavior of the condensation mass flux to the wall, the transient behavior of the surface temperature and the eventual steady state mass flux. Figure 1 shows a schematic diagram of the problem.

DIRECT SIMULATION TREATMENT FOR PURE VAPOR CONDENSATION

The problem of condensation of a pure vapor is simulated using the Direct Simulation Monte Carlo method originally introduced by Bird.^{3,4}

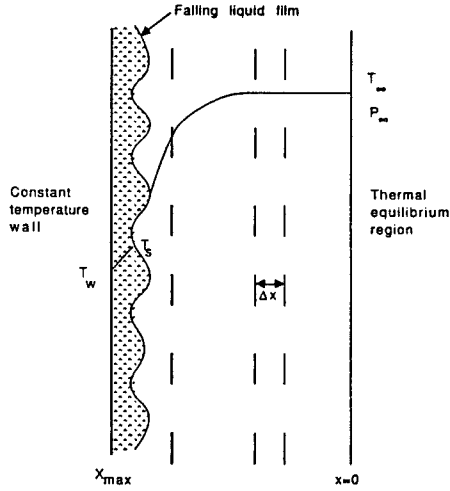


Fig. 1. A schematic diagram of the half space condensation problem in DSMC.

The flow field of condensing vapor is represented by a few thousand particles divided inside a number of computational cells.

There are a few major assumptions used in the modelling of the vapor condensation flux to the surface. These assumptions are listed below:

1. The vapor is considered an ideal gas;
2. Any particle of the vapor which collides with the surface of interface will condense ("stick") on the surface;
3. The liquid surface is also emitting particles which are in thermal equilibrium with the surface conditions;
4. The temperature of the surface interface between the condensate film and vapor is taken to be an axial average temperature determined from Nusselt's laminar film analysis over a particular length, L ;
5. The vapor molecules are hard sphere molecules;
6. The flow in the gas dynamics region is described by the Euler equilibrium flow.

To represent particles coming from the thermal equilibrium region an estimate of the relaxation distance of the flow field should be made, so that particles coming towards the wall from the gas dynamics region are in thermal equilibrium with the vapor bulk far from the interface. In the gas dynamics flow region the steady state mass continuity, the equation of motion, and the energy equation could be written as⁵

$$\rho u = \rho_{\infty} u_{\infty} , \quad (1)$$

$$P + \rho u^2 - \frac{4}{3} \mu \frac{du}{dx} = (P + \rho u^2)_{\infty} , \quad (2)$$

$$\begin{aligned} \rho u (C_p T + u^2/2) - k \frac{dT}{dx} - (4/3) \mu \frac{du}{dx} \\ = \rho_{\infty} u_{\infty} (C_p T + u^2/2)_{\infty} . \end{aligned} \quad (3)$$

where we follow the notation of Reference 5.

Defining

$$h = C_p T + u^2/2 ,$$

$$Pr = \mu C_p / k = 3/4 ,$$

$$z = (3/4) |J| \int_0^x \mu^{-1} dx ,$$

where μ = viscosity, $|J|$ = absolute mass flux, and $Pr = 3/4$ is valid for the majority of gases and vapors, and substituting into the energy equation (Eq. 3) yields

$$h + \frac{dh}{dz} = h_{\infty} . \quad (4)$$

The solution of this equation could be written in the form

$$h - h_{\infty} = (h_0 - h_{\infty}) e^{-z} . \quad (5)$$

For the value of $(h - h_{\infty})$ to approach zero, z should be on the order of 10. Assuming that μ does not change drastically from its average value $\bar{\mu}$, implies that

$$z = \frac{3}{4} \frac{|J|}{\bar{\mu}} x \sim 10 .$$

$|J|$ had been expressed in most of the mathematical models in the form of⁹

$$|J| \sim O(2.0) \frac{P_{\infty} - P_{sat}(T_w)}{\sqrt{2\pi R T_{\infty}}} .$$

$\bar{\mu}$ can also be expressed as⁴

$$\bar{\mu} \sim O(0.2 \sim 0.3) \rho_{\infty} \lambda_{\infty} \sqrt{2\pi R T_{\infty}}$$

where λ_{∞} is the mean free path of molecules, R = specific gas constant, and $O()$ means "order of".

Substituting the expression for $\bar{\mu}$ and $|J|$ in the approximate expression for z yields

$$z \sim \frac{30}{4} \frac{P_{\infty} - P_{\text{sat}}(T_w)}{2\pi\rho_{\infty}RT_{\infty}} \frac{x}{\lambda_{\infty}}.$$

Since $P_{\infty} = \rho_{\infty}RT_{\infty}$, and taking $z \sim 10$, the relaxation range is determined as

$$\frac{x_{\text{max}}}{\lambda_{\infty}} \sim 10.0 / \left[1 - \frac{P_{\text{sat}}}{P_{\infty}}\right]. \quad (6)$$

This equation gives an estimate for the relaxation distance as a first guess. This guess can be modified according to the results obtained in the analysis.

The relaxation range is subdivided into N cells parallel to the condensing surface, with each having a width Δx . The cell dimension should be very small such that the vapor properties may be regarded as spatially uniform with no variation in the macroscopic physical quantities. N_C molecules are generated randomly in each cell, so that the temperature in each cell is T_{∞} and the pressure is P_{∞} . The molecules are allowed to move and collide among themselves. The two processes are decoupled by computing collisions appropriate to a small time step, Δt_m , and then moving molecules through a distance appropriate to Δt_m and their instantaneous velocities. To evaluate the mass flux to the wall, the mass continuity Eq. (1) is applied at each time step to evaluate the mass flux, $(\rho_{\infty}u_{\infty})$, for the next time step.

Both Δt_m and Δx should satisfy the following conditions^{4,6,7}

- $\Delta t \ll t_{\infty}$,
- $\Delta x \ll \lambda_{\infty}$,
- $\frac{\Delta x}{\Delta t} \ll C_S$,

where

λ_{∞} = mean free path of molecules in the thermal equilibrium region

t_{∞} = mean collision time,

$$= \lambda_{\infty} / \sqrt{2RT_{\infty}},$$

and $C_S = \sqrt{2RT_{\infty}}$.

The three velocity components of each particle are generated initially from a normal distribution with a zero average and \sqrt{RT} standard deviation.

BOUNDARY CONDITIONS

The particles emitted from the wall are assumed to be in thermal equilibrium with the wall. Particles coming from the vapor bulk region, where the vapor satisfies Euler (or ideal) fluid equations with zero viscosity and zero thermal conductivity, are assumed to be in thermal equilibrium with the vapor far from the wall. Any vapor molecule which contacts the wall is going to condense.

The actual particle flux τ_{con} from the Eulerian region can be written as⁸

$$\tau_{\text{con}} = \frac{n_{\infty}RT_{\infty}}{\sqrt{2\pi RT_{\infty}}} \left[\exp(-G^2) + G\sqrt{\pi}(1 + \text{erf}(G)) \right], \quad (7)$$

where $G = |u_{\infty}/\sqrt{2RT_{\infty}}|$.

Thus the simulated number of particles emitted from the imaginary boundary limit between the Eulerian region and the represented field is

$$\left[\frac{\tau_{\text{con}} \Delta t}{\Delta x} \left(\frac{N_C}{n_{\infty}} \right) \right],$$

where

n_{∞} = actual number density of vapor in the Eulerian region, and

N_C = simulated number of molecules in the cell.

Similarly, for the evaporated particle flux from the wall, one gets^{8,10}

$$\tau_{\text{ev}} = \frac{n_S RT_S}{\sqrt{2\pi RT_S}}. \quad (8)$$

Thus, the number of simulated molecules emitted from the wall is

$$\left[\frac{\tau_{\text{ev}} \Delta t}{\Delta x} \left(\frac{N_C}{n_{\infty}} \right) \right].$$

The generated particle flux at both ends of the represented field should be in thermal equilibrium either with the gas bulk region or the wall.

To generate particle velocities at the boundaries, the following equations can be

used^{4,10}

$$\xi_y = \{-\ln(R_{f2})\}^{1/2} \cos(2\pi R_{f1})/\beta_i, \quad (9)$$

$$\xi_z = \{-\ln(R_{f2})\}^{1/2} \sin(2\pi R_{f1})/\beta_i, \quad (10)$$

$$\xi_x = x\sqrt{2RT_i} + u_i, \quad (11)$$

where i refers to either the surface (s), or the gas dynamics region (∞), x is the solution of the equation,¹⁰

$$A + \exp(-x^2) - \sqrt{\pi} G \operatorname{erf}(x) = 0,$$

A is given by

$$A = R_{f3} \{ \exp(-G^2) + \sqrt{\pi} G (\operatorname{erf}(G) + 1) \} \\ - \exp(-G^2) - \sqrt{\pi} G \operatorname{erf}(G).$$

β_j is $(\sqrt{2RT_i})^{-1}$, and R_{fj} , $j = 1,2,3$ are generated random numbers from the uniform distribution.

EVALUATION OF THE INTERFACE TEMPERATURE

The interface temperature is a function of the mass flux and the heat flux. An approximate estimation of the interface temperature can be evaluated using a modified Nusselt laminar film analysis. This assumption is valid if the condensing surface length is short or the film imposes a small resistance relative to the vapor, which is the situation in case of condensation at low pressure. Neglecting the heat flux due to conduction, and assuming that the condensation heat flux is independent of the height y , it can be shown that^{8,9}

$$T_s(y) - T_w = \left[\frac{3\mu_f Q^4}{k_f^3 h_{fg} \rho_f (\rho_f - \rho_g) g} \right]^{1/3} y^{1/3}.$$

Taking an average value of T_s over the total length of the condensation surface, one gets

$$\bar{T}_s = T_w + \left[\frac{81}{64} \frac{\mu_f Q^4 L}{k_f^3 h_{fg} \rho_f (\rho_f - \rho_g) g} \right]^{1/3}, \quad (12)$$

where

μ_f = viscosity of the liquid,

k_f = thermal conductivity of the liquid,
 h_{fg} = latent heat of vaporization,
 ρ_f, ρ_g = density of liquid and vapor respectively,
 Q = heat flux per unit area,
 $T_s(y)$ = temperature of liquid at the interface,
 T_w = constant temperature of the solid surface,
 and L = condensate surface axial height.

RESULTS AND DISCUSSION

The DSMC code results were compared to experimental data available for mercury condensation on a vertical plane square (side 40 mm) nickel-plated copper surface.⁹ This data was the only data applicable to the conditions of a monatomic gas condensing at low pressure. The vapor temperatures range from 419 K up to 495 K with temperature difference between the plate and vapor ranging from 9.7 K to 30.8 K. The mercury vapor was saturated vapor at saturation pressure corresponding to its temperature. Nine experiments were simulated out of the twenty experiments. Only the tests without flow parallel to the surface of condensation were considered. The results were compared with the experiment and some of the available theoretical models casted in a form using a dimensionless variable ζ introduced by Necmi and Rose⁹ which is described later in Section B.

Figure 2 shows the pressure and number density as a function of position for experiment #7 in the same reference as an example of the simulation output results. Both the pressure and the number density are normalized to their values in the gas dynamics region. The standard deviation in the output is less than 7% of its average value. The number of simulated flow particles per cell in this experiment is 200 particles/cell. Figure 3 shows the average fluid velocity in the gas dynamics region and the condensate surface temperature as a function of time for the same experiment. The standard deviation values in both u_∞ and T_s are less than 2% of their average value.

A. Comparison With Experiment

The comparison of the results with experiments is shown in Table 1. The velocity of fluid in the gas dynamics region, u_∞ , is an indication about the mass flux since the mass flux J is given as $J = \rho_\infty u_\infty$ and ρ_∞ is the density of the vapor in the gas dynamics region (GDR). It shows that the DSMC model overestimates the experimental steady state mass flux by a fairly constant factor; i.e., $(u_{ex}/u_{th})_\infty \sim 0.71$ over the range of Mach numbers, Ma , covered by the experiments. Figure 4 shows the experimental results and the DSMC results of the dimensionless number ζ defined in Reference 9 and Eqs. (a-e) of Section B. The mass flux estimated from the DSMC model is higher than that estimated from the experimental

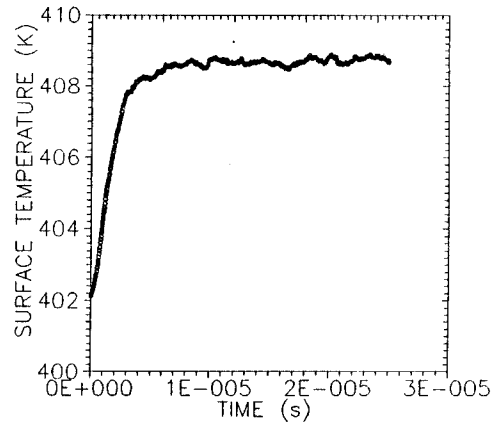
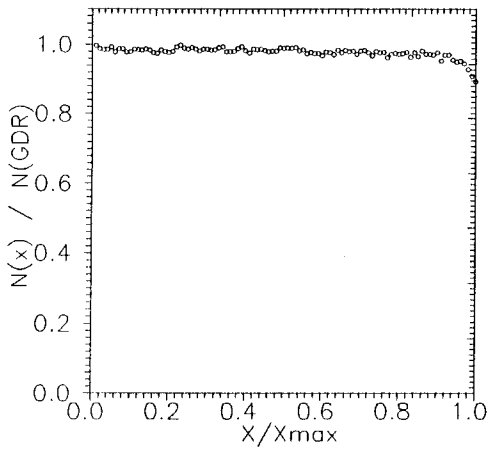
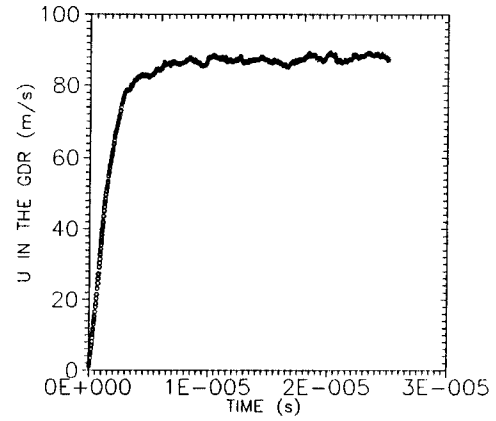
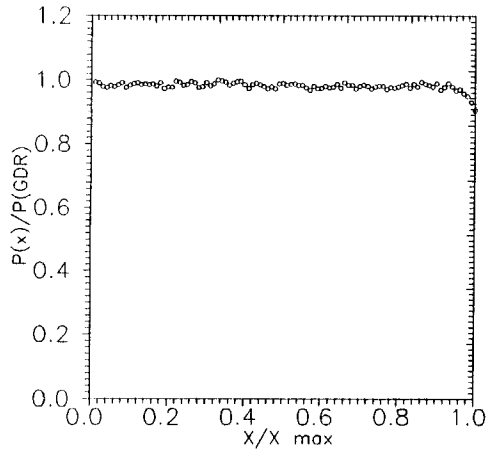


Fig. 2. Calculated pressure and number density as a function of position for experiment #7.

Fig. 3. Change of average fluid velocity, u_{∞} , and condensate surface temperature with time for experiment #7.

Table 1. Comparison with Experiment

Ex #	T_{∞} (K)	T_w (K)	ΔT (K)	T_s (K)	Ma_{ex}	Ma_{th}	$\frac{Ma_{ex}}{Ma_{th}}$	$(u_{\infty})_{ex}$ (m/s)	$(u_{\infty})_{th}$ (m/s)
2	419.3	399.3	20.0	401.6	0.273	0.357	0.77	47	61.3
3	433.4	420.9	12.5	422.9	0.148	0.204	0.73	26	35.6
7	432.9	402.1	30.8	408.8	0.364	0.509	0.72	63	88.1
9	449.4	439.0	10.4	440.9	0.108	0.145	0.74	19	25.8
12	449.1	427.0	22.1	432.8	0.217	0.318	0.69	39	56.6
16	462.3	449.7	12.6	452.3	0.114	0.157	0.71	20	28.3
22	462.0	449.3	12.7	453.4	0.111	0.158	0.70	20	28.5
25	495.0	484.6	10.4	488.5	0.052	0.075	0.69	10	14.4
27	493.8	481.3	12.5	486.0	0.065	0.093	0.69	12	17.3

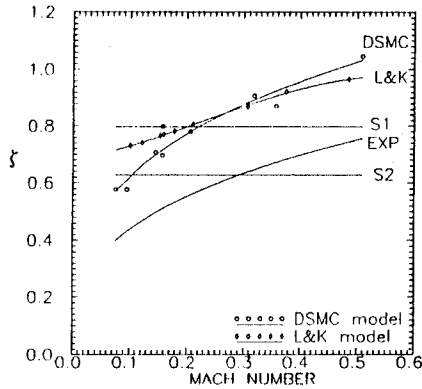


Fig. 4. The variation of ζ with Mach number for the experiment and different theoretical models.

fitting curve given in Reference 9. The standard deviation of the steady state mass flux estimated using the DSMC code was on the order of 3.0% due to the discretization of time steps, cell dimensions and the limitation on the number of particles used for simulation. The overestimation of the DSMC method used may be related to the following assumptions in the model:

1. The assumption of a unity condensation coefficient. The unity sticking probability is a crude assumption in the model. Such a probability is related to the temperature of the vapor and the nature of the surface of condensation, and it should be taken into consideration that it would be below 1.
2. The inadequacy of the hard sphere model to represent the molecular potential during molecular interactions.
3. Neglecting the temperature gradient in the vapor reported by the experimental paper.
4. Neglecting the temperature gradient along the interface by using the average temperature from the modified Nusselt analysis to represent the interface temperature.
5. Traces of a noncondensable gas in the experiment.

B. Comparison With Theoretical Models

In the course of comparing DSMC method to other theoretical models, the following models are going to be introduced:

1. Schrage linear model (S1).
2. Schrage monatomic linearized analysis (S2).
3. Labuntsov and Muratova (L&M).
4. Labuntsov and Kryukov model (L&K).
5. Crude kinetic theory (K.T.).

All of these analytical models can be casted in the form

$$J = \zeta \frac{P_{\infty} - P_s}{\sqrt{RT_{\infty}}}$$

where ζ is a dimensionless number that varies from one analytical model to another. For the previous analytical models ζ takes the form

$$(a) \text{ S1} : \zeta = \left(\frac{2\sigma}{2-\sigma}\right) / \sqrt{2\pi}$$

$$(b) \text{ S2} : \zeta = \sqrt{\pi/8} = 0.627$$

$$(c) \text{ L\&M} : \zeta = \left(\frac{2\sigma}{2-0.798\sigma}\right) / \sqrt{2\pi}$$

$$(d) \text{ L\&K} : \zeta = \frac{1.67}{\sqrt{2\pi}} \left[1 + 0.5151 \ln\left(\frac{P_{\infty}}{P_s} \sqrt{\frac{T_{\infty}}{T_s}}\right)\right]$$

$$(e) \text{ Crude K.T.} : \zeta = \frac{P_{\infty} - P_s \sqrt{T_{\infty}/T_s}}{\sqrt{2\pi}(P_{\infty} - P_s)}$$

where σ = condensation coefficient = 1.

The comparison with these theoretical models is given in Tables 2 and 3. Table 2 shows the estimated values of the fluid velocity, u_{∞} , to the condensing surface using different models. The estimated values from the DSMC method have a standard deviation of less than 2%. The surface temperature is evaluated through the course of simulation using the modified Nusselt analysis.

Table 3 shows the value of $(u_{ex}/u_{th})_{\infty}$ for these models with the value estimated using the DSMC method. The range of this ratio for different models through simulated experiments range are,

$$\text{S1} : 0.48 \leq (u_{ex}/u_{th})_{\infty} \leq 0.94$$

$$\text{S2} : 0.64 \leq (u_{ex}/u_{th})_{\infty} \leq 1.19$$

$$\text{L\&M} : 0.60 \leq (u_{ex}/u_{th})_{\infty} \leq 1.13$$

$$\text{L\&K} : 0.54 \leq (u_{ex}/u_{th})_{\infty} \leq 0.75$$

$$\text{K.T.} : 1.02 \leq (u_{ex}/u_{th})_{\infty} \leq 1.91$$

$$\text{DSMC} : 0.69 \leq (u_{ex}/u_{th})_{\infty} \leq 0.77$$

From these ranges it is clear that the DSMC method is the model which has the most consistent representation of the qualitative trends and behavior of the experimental data. The Crude kinetic theory is the worst of these models because it assumes complete thermal equilibrium near the wall. The value of ζ has been plotted versus the Mach number for different experiments in Figure 4. From that figure it is clear that the constant ζ models S1, S2, and L&M were not able to predict the variation of ζ with Mach number, while the L&K and DSMC models were able to predict ζ behavior with Mach number. For small Mach numbers the

Table 2. Estimated values of fluid velocity, u_{∞} , to the condensate surface using different theoretical models in (m/s).

Ex #	T_v (K)	T_s (K)	S1	S2	L&M	KT	L&K	DSMC	EX
2	419.3	401.6	55.6	43.7	46.2	27.2	63.9	61.3	47
3	433.4	422.9	36.3	28.5	30.2	17.7	36.6	35.6	26
7	432.9	408.8	67.2	52.8	56.0	33.0	84.0	88.1	63
9	449.4	440.9	29.1	22.9	24.3	14.2	28.1	25.8	19
12	449.1	432.8	49.8	39.1	41.4	24.3	54.2	56.6	39
16	462.3	452.3	32.4	25.5	27.0	15.8	31.8	28.3	20
22	462.0	453.4	28.5	22.4	23.7	13.9	27.4	28.5	20
25	495.0	488.5	20.2	15.8	16.8	9.8	18.5	14.4	10
27	493.8	486.0	23.9	18.8	19.9	11.6	22.3	17.3	12

Table 3. Values of $(u_{ex}/u_{th})_{\infty}$ evaluated using different theoretical models.

Ex #	S1	S2	L&M	L&K	KT	DSMC
2	0.85	1.08	1.02	0.74	1.72	0.77
3	0.72	0.91	0.86	0.71	1.47	0.73
7	0.94	1.19	1.13	0.75	1.91	0.72
9	0.65	0.83	0.78	0.68	1.34	0.74
12	0.78	1.00	0.94	0.72	1.60	0.69
16	0.62	0.78	0.74	0.63	1.27	0.71
22	0.70	0.89	0.84	0.73	1.44	0.70
25	0.48	0.63	0.60	0.54	1.02	0.69
27	0.50	0.64	0.60	0.54	1.04	0.69

L&K model overestimates the mass flux by nearly a factor of 2. This may be due to the underestimation of collisions near the condensing surface where the 13-grad moment distribution is assumed. The DSMC method gives a consistent and almost constant value for the ratio $(u_{ex}/u_{th})_{\infty}$.

CONCLUSION AND FURTHER WORK

The DSMC method can be used to represent condensation at low pressures with a reasonable standard deviation. It has the ability to predict the condensation mass flux, although the data is overestimated by 20-30%. The unity condensation coefficient and the hard sphere potential assumption are the most suspected reasons for the overestimation. The use of other models to represent the molecular potential to compare the effect of different molecular potentials is strongly suggested. Also, the dependency of the condensation coefficient on the particle energy should be taken into

consideration. The DSMC method is being used now to predict the effect of a noncondensable gas on condensation.

ACKNOWLEDGMENT

This work has been funded by the U.S. Department of Energy through Lawrence Livermore National Laboratory.

REFERENCES

1. B. BADGER et al., "HIBALL- A Conceptual Heavy Ion Beam Driven Fusion Reactor Study," University of Wisconsin Fusion Technology Institute Report UWFD-450 (1981).
2. M.L. CORRADINI et al., "Liquid Metal Condensation in the Cavity of HIBALL Heavy Ion Fusion Reactor," Nuclear Engineering & Design/Fusion 3, p.47 (1985).
3. G.A. BIRD, "Direct Simulation Monte Carlo Method- Current Status and Prospects," Rarefied Gas Dynamics, V-1, p.85, (1969).
4. G.A. BIRD, "Molecular Gas Dynamics," Clarendon Press, Oxford, (1976).
5. D.A. LABUNTSOV and A.P. KRYUKOV, "Analysis of Intensive Evaporation and Condensation," International Journal of Heat and Mass Transfer, V-22, p.989, (1979).
6. G.A. BIRD, "Direct Simulation of Gas Flows at the Molecular Level," Presented at World Congress On Computational Mechanics, (1986).
7. E. KLEIN and Y. STEPHAN, "The Direct Simulation Monte Carlo Applied to Dilute Gas Dynamics," Monte Carlo Methods and Applications; Proceedings of the Joint Los

Alamos National Laboratory-Commissariat
a L'Energie Atomique Meeting held at
Cadarache Castle, Provence, France, April
22-26, 1985.

8. J. COLLIER, "Convective Boiling and Condensation, Ch.10, McGraw Hill, NY, (1980).
9. S. NECMI and J.W. ROSE, "Film Condensation of Mercury," International Journal of Heat and Mass Transfer, V-19, p.1245, (1979).
10. M. ELAFIFY, "Condensation of Liquid Metals Under Low Pressures," Ph.D. Thesis, Nuclear Engineering and Engineering Physics, UW-Madison (1988).